



## The relationship among earthquake location, magnetization, and subsurface temperature beneath the Taiwan areas

Qiang Zu<sup>a</sup>, Chieh-Hung Chen<sup>a,b,\*</sup>, Chun-Rong Chen<sup>c</sup>, Shuang Liu<sup>a</sup>, Horng-Yuan Yen<sup>d</sup>

<sup>a</sup> Institute of Geophysics and Geomatics, China University of Geosciences, Wuhan, China

<sup>b</sup> State Key Laboratory of Geological Processes and Mineral Resources, Institute of Geophysics and Geomatics, China University of Geosciences, Wuhan, China

<sup>c</sup> Graduate Institute of Space Science, National Central University, Taoyuan, Taiwan

<sup>d</sup> Department of Earth Sciences, National Central University, Zhongli 320, Taiwan

### ARTICLE INFO

#### Keywords:

Aseismic region  
Geomagnetic anomaly  
Magnetization inversion

### ABSTRACT

Earthquake locations are mainly determined by the strength of the rocks and the subsurface temperature. However, other geophysical factors may play a role in the localization of earthquakes. Noting that the anomaly in magnetic intensity is positive in the aseismic regions of Taiwan, we investigate the spatial correlation between the magnetization and earthquake locations. We estimate the magnetization from the surface down to the depth of 45 km from the magnetic intensity map at the surface of Taiwan. Focusing on the regions where the rocks are brittle and the temperature less than 450 °C, we find that earthquakes tend to occur in the strata with relatively-low magnetization. Conversely and in agreement with the observation that rocks undergo ductile deformation when the temperature is greater than 450 °C, we find that the subsurface temperature is the key determinant for the localization of earthquakes within regions where the temperature is higher than 450 °C. Magnetization should be considered as an additional parameter that governs the earthquake locations.

### 1. Introduction

Taiwan is located at the collisional plate boundary on the western margin of the Pacific Ocean (Hsu and Sibuet, 1995; Lacombe et al., 2001; Lin et al., 2003). The Philippine Sea Plate interacts strongly with the Eurasian Plate, forming two subduction zones in the northeastern and southwestern parts of Taiwan. These interactions cause a great number of earthquakes in the surrounding area, which is well known globally for its high-seismicity. On average, three or four earthquakes with magnitude  $\geq 6$  strike this area each year (Chang et al., 2016). To improve the earthquake catalog in Taiwan, the number of seismometers increases with time. A total of 192,548 earthquakes were detected close to Taiwan by using dense seismic arrays comprising modern seismometers between 2013 and 2017 that can be retrieved from the Central Weather Bureau, Taiwan. We plotted those earthquakes with magnitudes ranging from 0.03 to 7.69 occurring between 1991 and 2017 in Fig. 1a. It can be found that the spatial distribution of seismicity is uneven in the land areas of Taiwan. Four aseismic regions (Kuan-Yin (KY), Pei-Kang (PK), Kao-Ping (KP), and the Southern segment of the Central Range (SC); Yen et al., 2009) with relatively-low seismicity can be shown in the map (Fig. 1a). In general, seismicity activities are supposed

to be dominated by the strength of rocks (Whitcomb et al., 1973; Leary, 1997; Singh et al., 2011; Tarasov and Randolph, 2011; Bassett and Watts, 2015; Ikari et al., 2015). Rocks beneath aseismic regions are generally considered to be harder than their vicinity.

Various geophysical prospection methods, such as gravity, magnetic, electrical, and seismic, have been employed to investigate complex underground geological structures (Tsai et al., 1974; Yen et al., 1998; Chen and Chen, 2000; Chen et al., 2001; Wang et al., 2002). An island-wide magnetic prospection was carried out in Taiwan in 2005 (Yen et al., 2009). A total of 6063 observation points was processed, mainly along secondary roads with a spatial interval of approximately 2 km in the plain areas and 5 km in the mountainous regions. A magnetic anomaly map of Taiwan (Yen et al., 2009; Fig. 1b) was obtained from the field prospection data using the standard protocols (Regan and Cain, 1975; Barton, 1997). The magnetic anomaly in Taiwan mainly ranges between  $-650$  nT and  $400$  nT. The positive magnetic anomaly is roughly distributed around the northern (I), central (II), and southwestern (III) regions, the southern part of the Central Range (IV) and the eastern margin (V) (Fig. 1b). The positive anomaly is generally identified by the remains of igneous, iron-rich sedimentary rocks and intrusive magma (Yu and Tsai, 1979; Deschamps et al., 2000; Tong et al., 2008). In

\* Corresponding author at: Institute of Geophysics and Geomatics, China University of Geosciences, Wuhan, Hubei 430074, China.

E-mail address: [nononochchen@gmail.com](mailto:nononochchen@gmail.com) (C.-H. Chen).

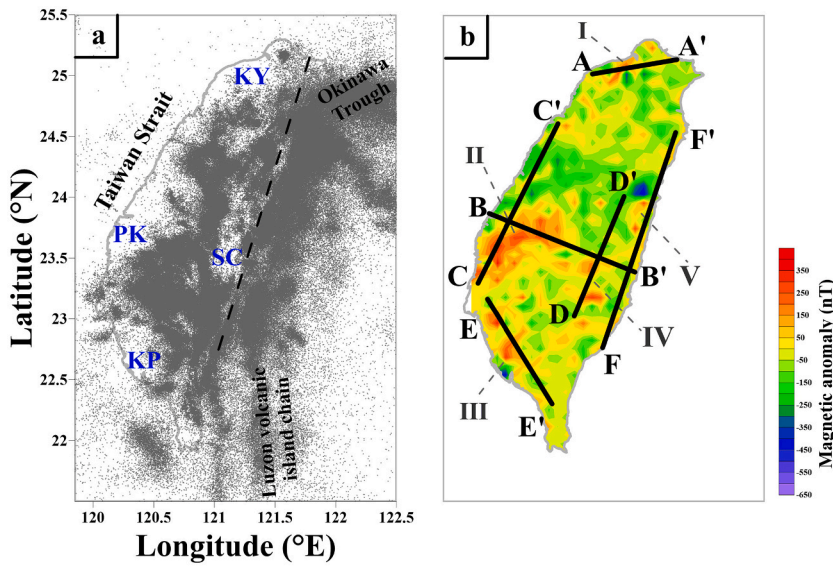


**Fig. 1.** Seismicity and magnetic anomaly map of the Taiwan area. The seismicity map is shown in (a). Gray dots indicate the epicenters of earthquakes with magnitudes ranging from 0.03 to 7.69 occurring during 1991–2017 as reported by the Central Weather Bureau, Taiwan. Locations of four aseismic regions (Kuan-Yin (KY), Pei-Kang (PK), Kao-Ping (KP) and the Southern segment of the Central Range (SC)) are marked by blue text. The dotted line is the dividing line between the east and west of Taiwan. The magnetic anomaly map in Taiwan Island is shown in (b). Five profiles (AA', BB', CC', DD' and EE') cross the aseismic regions and the FF' profile is located along the eastern margin of Taiwan Island over the suture zone. Locations of the five positive magnetic anomalies are indicated by I–V with dashed lines. (For interpretation of the references to colour in this figure legend, the reader is referred to the web version of this article.)

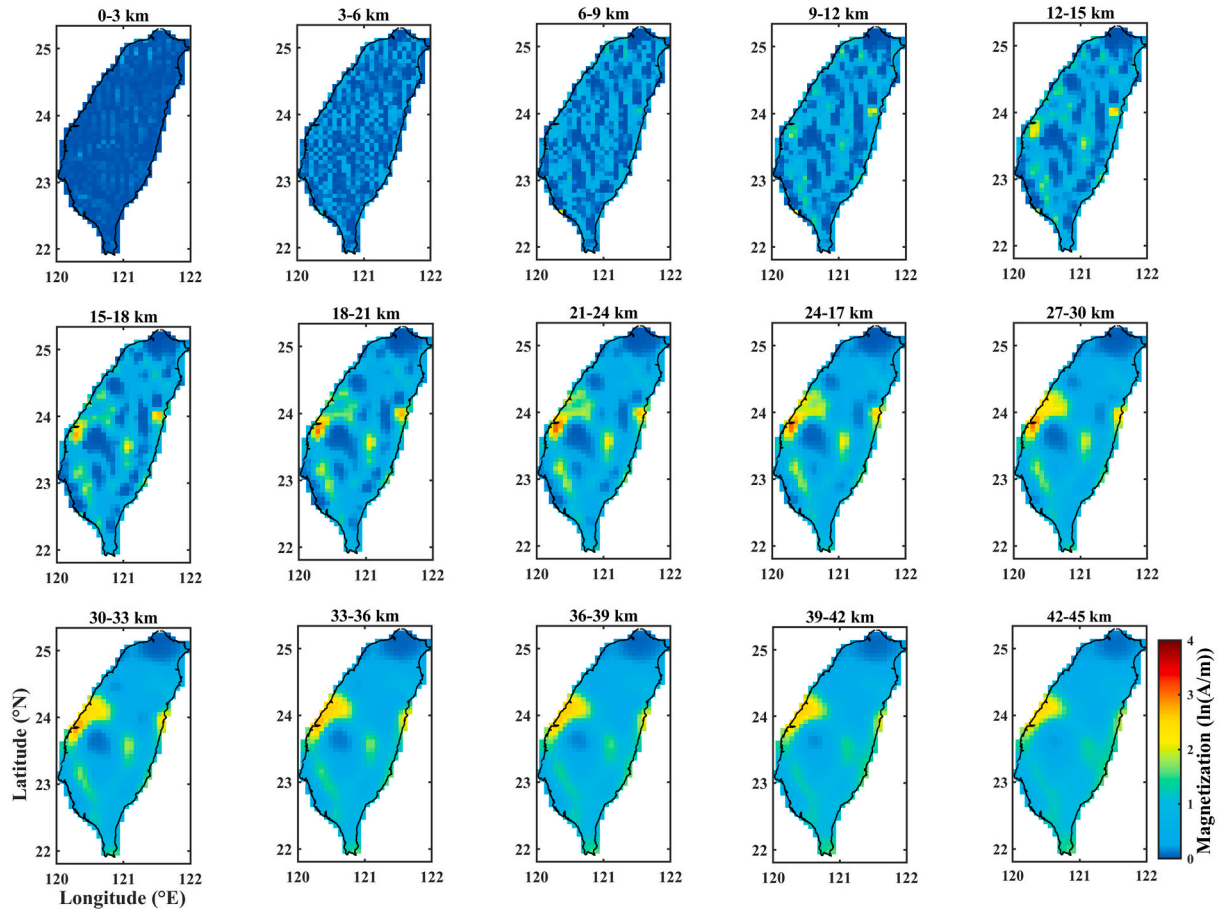


**Fig. 2.** The horizontal slices of the 3-D magnetization distribution from shallow to deep depths with an interval of 3 km. The colour denotes the intensity of the magnetization within the underground grids.

contrast, the negative geomagnetic anomaly is located in the plain areas and in the northeastern part of Taiwan resulting from the presence of sediment. We compared the seismicity map with the magnetic anomaly map and found a spatial correlation between the aseismic regions (Fig. 1a) and the positive magnetic anomaly (Fig. 1b). Hsu et al. (2008) inverted the magnetic anomaly to obtain the equivalent crustal

magnetization distribution in Taiwan, and found that earthquakes occurred in areas with relatively-low magnetization. Meanwhile, the correlation (i.e., a rough overlap between the aseismic regions and the positive magnetic anomaly) can also be found in Tang-Shan, Luan-Xian, Sichuan Basin, and Japan Island (Hasegawa and Yamamoto, 1994; Zhang et al., 1995a, 1995b; Nakatsuka et al., 2005). These suggest that

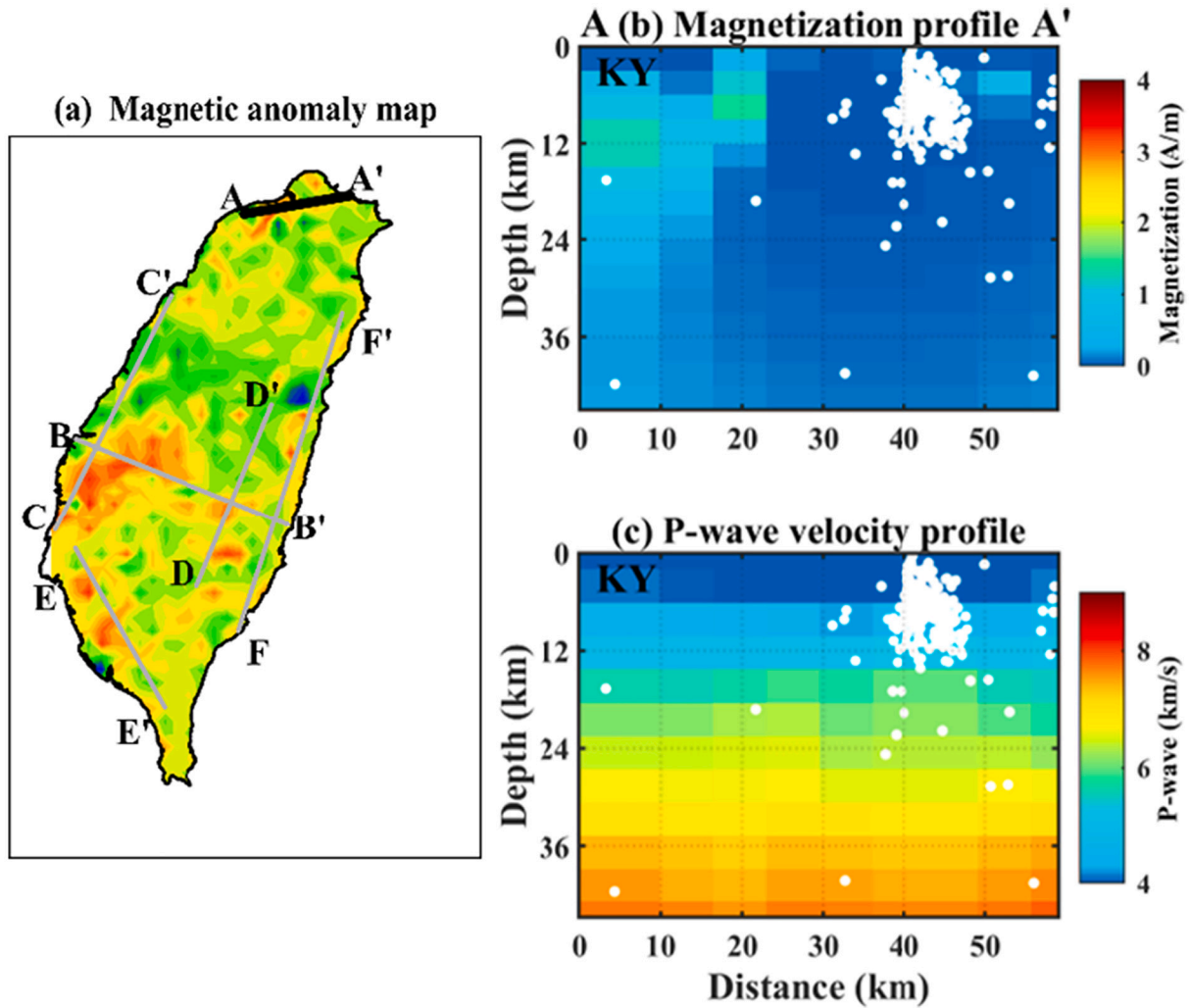


Fig. 3. Magnetization and P-wave velocity along the cross-section AA'. White dots indicate the hypocenters of earthquakes with magnitudes  $\geq 2$  and within a distance of 5 km perpendicular to the profile.

Table 1

Formation ages of magnetic materials in Taiwan.

	Ages (Ma)	References
KY	Palaeogene (~66–23)	Lin et al. (2003)
PK	Palaeogene (~66–23)	Hsu et al. (1998)
KP	Miocene (~23–12)	Nagel et al. (2013)
SC	Neocene (~5–0)	Lin (2000)
Eastern margin	Neocene (~6.5–0)	Sibuet and Hsu (1997)

magnetization would be an additional parameter that is related to the earthquake locations.

In this study, we construct a 3-D magnetization structure beneath the study area (from latitude 21.8–25.3° N and longitude 120.0–122.0° E) by using the inversion method (Li and Oldenburg, 1996, 2003). Five profiles that cross the four aseismic regions are selected to reveal the relationship between the underlying magnetization structure and the location of earthquakes. In addition, the sixth profile, which is located along the suture zone between the Philippine Sea Plate and the Eurasian Plate, is selected to clarify the relationship between seismicity and the magnetization structure under distinct geological conditions.

## 2. Methodology

The inversion method proposed in Li and Oldenburg (1996, 2003) is utilized in this study for investigating the distribution of magnetization beneath the study area. The inversion work begins from a homogeneous initial model, which was comprised of  $56 \times 29 \times 15$  grids with a size of  $7 \times 7 \times 3 \text{ km}^3$ , and was set to be a zero model because the distribution of the underground magnetization was unclear. The thickness of the initial model was determined to be 45 km to fully cover the distinct Curie point depths (Lin, 2000; Simoes et al., 2007; Hsieh et al., 2014; Tang et al., 2019). The differences between the observation data and the forward data contributed by the initial model are shown in Fig. S1.

The magnetic anomaly on the Earth's surface caused by underground magnetization can be computed by.

$$MA_n = d_{nm} \cdot M_m \quad (1)$$

where  $MA_n$  is the magnetic anomaly (nT) in the  $n_{th}$  datum on the Earth's surface obtained from magnetic prospection using standard correction methods,  $M_m$  is the magnetization (A/m) in the  $m_{th}$  grid, and  $d_{nm}$  quantifies the contribution of a unit of magnetization in the  $m_{th}$  grid to the  $n_{th}$  datum (Li and Oldenburg, 1996; Luo and Yao, 2007).

We defined a misfit function in Eq. (2) using the  $L_2$  norm of the difference between the observation ( $MA_n$ ) and the simulation ( $d_{nm} \cdot M_m$ ),

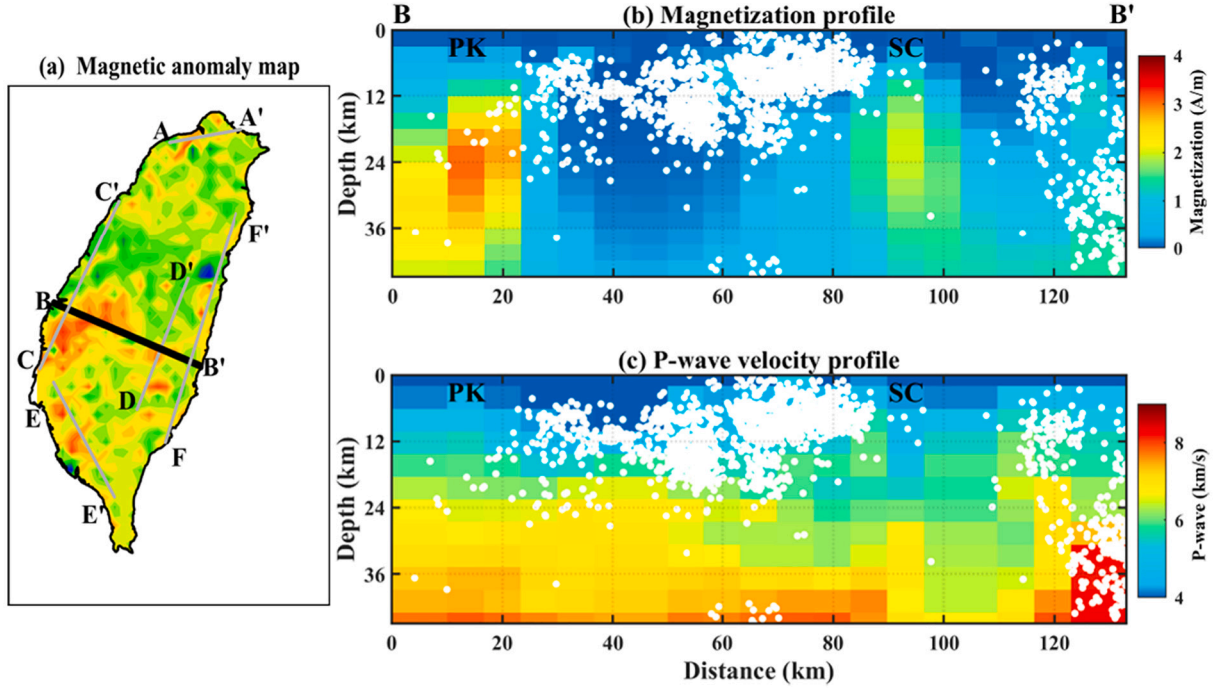


Fig. 4. Magnetization and P-wave velocity along the cross-section BB'. White dots indicate the hypocenters of earthquakes with magnitudes  $\geq 2$  and within a distance of 5 km perpendicular to the profile.

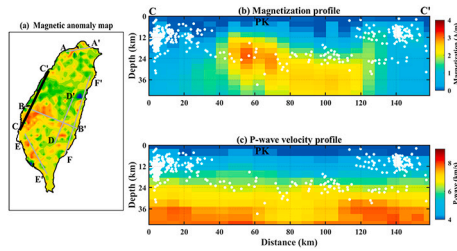


Fig. 5. Magnetization and P-wave velocity along the cross-section CC'. White dots indicate the hypocenters of earthquakes with magnitudes  $\geq 2$  and within a distance of 5 km perpendicular to the profile.

$$\Phi = \|W_n(d_{mm} \cdot M_m - MA_n)\|_2^2 \quad (2)$$

where  $W_n$  is a diagonal matrix, whose  $n_{th}$  element is  $1/\sigma_n$  and  $\sigma_n$  is the standard deviation of the  $n_{th}$  datum.  $W_n$  is generally set to be a unit matrix due to the unknown deviation of the magnetic anomaly. A minimum model constraint ( $\|Z(M_m - M_{ref})\|_2^2$ ) in Eq. (3) was applied to suppress the non-uniqueness problem in the inversion process. We then rewrote Eq. (2) as

$$\Phi = \|W_n(d_{mm} \cdot M_m - MA_n)\|_2^2 + \mu \cdot \|Z(M_m - M_{ref})\|_2^2 \quad (3)$$

where  $\mu$  is the regularization factor utilized to balance the weighting between the data misfit and model constraint, the  $M_{ref}$  is a reference model, and  $Z$  is the depth weighting matrix that given by:

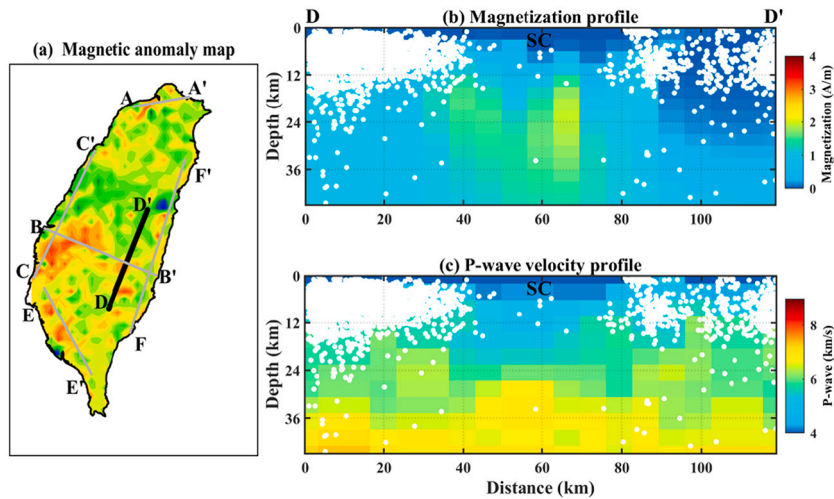


Fig. 6. Magnetization and P-wave velocity along the cross-section DD'. White dots indicate the hypocenters of earthquakes with magnitudes  $\geq 2$  and within a distance of 5 km perpendicular to the profile.

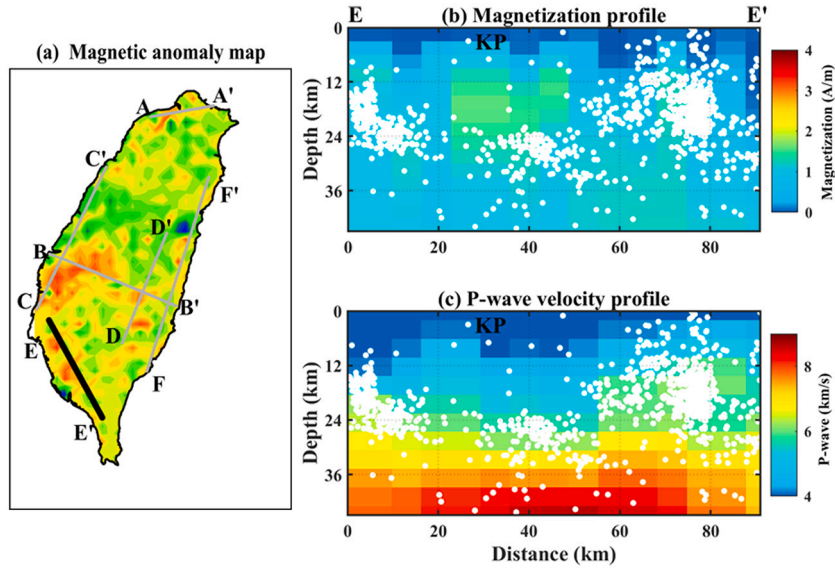


Fig. 7. Magnetization and P-wave velocity along the cross-section EE'. White dots indicate the hypocenters of earthquakes with magnitudes  $\geq 2$  and within a distance of 5 km perpendicular to the profile.

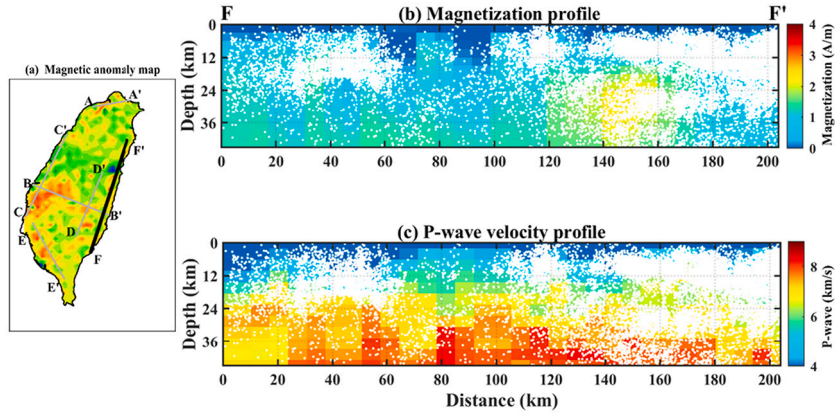


Fig. 8. Magnetization and P-wave velocity along the cross-section FF'. White dots indicate the hypocenters of earthquakes with magnitudes  $\geq 2$  and within a distance of 5 km perpendicular to the profile.

$$Z = \frac{1}{(z_m + z_0)^{(3/2)}} \quad (4)$$

Where  $z_m$  is the center depth of the  $m_{th}$  grid;  $z_0$  is a constant which is set to be zero in this study. The depth weighting matrix is used to avoid the over-concentration of the magnetization close to Earth's surface (Li and Oldenburg, 1996). The reference model ( $M_{ref}$ ) is given by a homogeneous model of zero to avoid the effect of an artificial factor due to subjective uncertainty. In addition, we constrained the magnetization of the underlying materials by using positive values through the logarithmic barrier method (Li and Oldenburg, 2003; Li et al., 2018) to adapt nature. The formula was then rewritten as

$$\Phi = \|W_n(d_{nm} \cdot M_m - MA_n)\|_2^2 + \mu \cdot \|Z(M_m - M_{ref})\|_2^2 - 2\lambda(\ln(M_m) + \ln(M_{max} - M_m)) \quad (5)$$

where  $\lambda$  is the barrier parameter and  $M_{max}$  is the limitation of the magnetization maximum in each grid. The Gauss-Newton method was utilized to find the optimal solutions of Eq. (5) by minimizing  $\Phi$  through the iteration process. The preconditioned conjugate gradient (PCG) method (Pilkington, 1997; Li and Oldenburg, 2003) was used to determine the changes in  $M_m$  during the iterative process.

In practice, the selection of the regularization factor ( $\mu$ ) at Eq. (5) is more flexible that often dominates the depth of magnetization in inversion results. Hansen and O'Leary (1993) used the L-curve criterion to choose an optimal regularization factor. The L-curve is constructed by the misfit functions versus to the minimum models that are computed by using a series of regularization factors. The optimal regularization factor is determined by the inflection point of the L-curve. In this study,  $\mu$  is given from 150 to 3000 to construct the L-curve and the optimal regularization factor is determined as 500 (Fig. S2).

### 3. Inversion results

The 3-D magnetization structure was obtained after 40 iterations (Fig. S3) with the Gauss-Newton method. The differences between the magnetic anomaly calculated from the inversion results and the observation data are generally ranging from  $-0.3$  nT to  $0.2$  nT (Figs. S4 and S5). This suggests that the inversion results do show a potential distribution of the magnetization beneath the area around Taiwan. Fifteen horizontal slices of the 3-D magnetization structure from the surface to the depth of 45 km with an interval of 3 km are shown in Fig. 2. Materials with a high level of magnetization cluster beneath the KY, PK, KP, SC, and the eastern margin of Taiwan, at a depth ranging from about 6

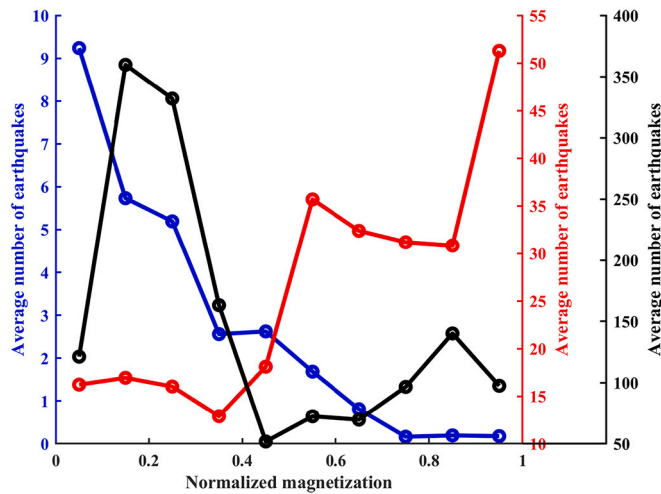


**Fig. 9.** The relationship between the average number of earthquakes and the normalized magnetization in Taiwan. The blue, red and black lines show the relationship in the west and the east of Taiwan, and along the FF' profile, respectively. (For interpretation of the references to colour in this figure legend, the reader is referred to the web version of this article.)

km to 36 km. The aseismic regions located above the highly magnetized materials confirms the findings through comparison between Figs. 1 and 2.

The KY high region associated with the AA' profile is shown in Fig. 3. The KY high region was forged in the Palaeogene (Table 1), due to the uplift of the magnetic basement (Lin et al., 2003). Earthquakes around the AA' profile locate close to the volcanic neck and magma reservoir of the Tatun Volcano Group (Konstantinou et al., 2007), which is far from the KY region. The relatively-high level of magnetization mainly distributes at both sides of the earthquake cluster between 3 km and 15 km in depth (Fig. 3b). The P-wave velocity increases with the depth of the AA' profile (Fig. 3c). No significant lateral change in the P-wave velocity can be found from the AA' profile. Earthquake locations are difficult to be directly referred to changes in the P-wave velocity.

The BB' (Fig. 4) and CC' (Fig. 5) profiles cross the PK aseismic region in the west of Taiwan. The PK basement high is over the eastern end of the positive magnetic anomaly belt from the Taiwan Strait (Hsu et al.,

1998; Doo et al., 2015). The materials with a relatively-high level of magnetization in the PK aseismic region locate at depths from 12 km down to about 36 km (Figs. 4b and 5b). The highly magnetized materials are referred to igneous rocks that were formed during the Paleocene (Lee and Din, 1993; Lee, 1996, also listed in Table 1). Locations of the earthquakes are distant from these magnetic materials. The strong basement rocks of the PK region can be characterized by the relatively-high level of P-wave velocity (Figs. 4c and 5c). Earthquakes usually occur around the depths with the P-wave velocity of ~5 km/s due to the series of décollements at the shallow and friable sediment layers formed by orogeny in the west of Taiwan (Suppe, 1981).

The underground magnetization distribution, earthquake locations, and P-wave velocity structure beneath the SC region are shown in the BB' and DD' profiles (Figs. 4 and 6). Figs. 4b and 6b reveal that the relatively-high level magnetization roughly distributes at depths from 12 km to 30 km underlying the SC region. The existence of the relatively-high level magnetization agrees with the magnetic anomaly map (Yen et al., 2009; Chen et al., 2021). Few earthquakes locate in the region with highly magnetic materials. The SC region is composed of the Paleogene metamorphic rock basement (Yu et al., 1997). The P-wave velocity underlying the SC region shows a relatively-low level that ranges from about 4 km/s to 7 km/s. Earthquakes distributions locate at shallow depths (3 km–18 km) with the P-wave velocity of about 5 km/s to 6 km/s (Fig. 6c).

The southwest Taiwan around the EE' profile (Fig. 7) is filled with thick sediments formed in Miocene (Nagel et al., 2013; also listed in Table 1). The materials with relatively-high magnetization beneath the KP aseismic region in southwestern Taiwan distribute at depths from 9 km to 24 km (Fig. 7b). Hypocenters of earthquakes are located away from regions with high-level magnetization. Horng et al. (1992) reported that greigite/pyrrhotite-bearing materials exist beneath the KP region, and the relatively-high level of magnetization is caused by these magnetic materials. The low P-wave velocity is supposed to be related to the thickly sedimentary strata around the KP region (Fig. 7c). Earthquakes seem to occur around strata with the P-wave velocity of 6 km/s (Fig. 7c).

In short, the four aseismic regions consist of strong basements or thick sediments. Earthquakes roughly locate in areas with a relatively-low level of P-wave velocity. However, earthquakes cluster in a particular region beneath the AA' profile in Fig. 3 and in the two places underlying the CC' and DD' profiles in Figs. 5 and 6 without significant

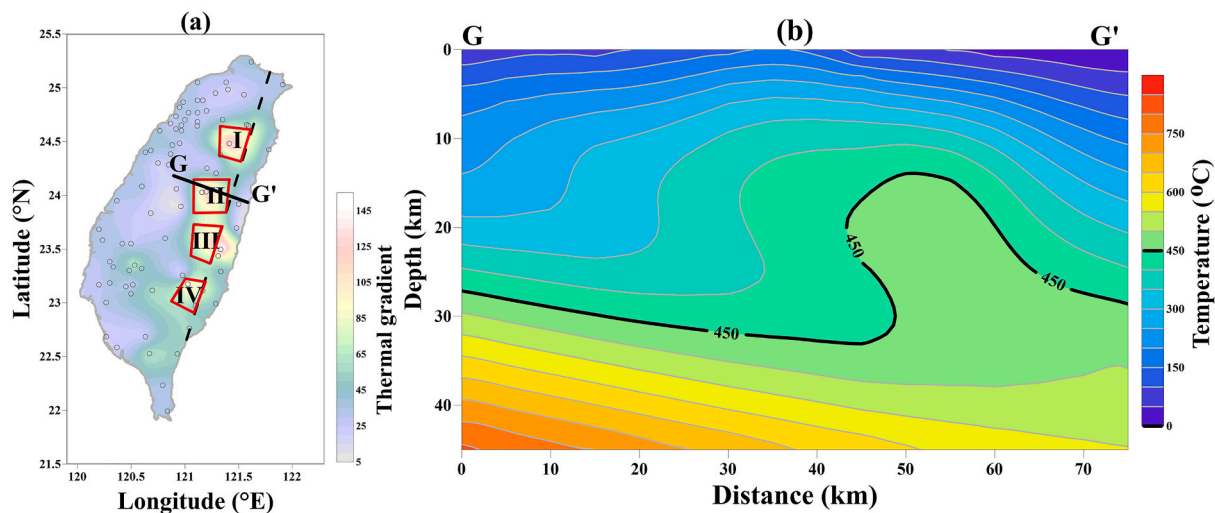


**Fig. 10.** The thermal gradients (Lee and Cheng, 1986) in the Taiwan area are shown in (a). The open circles indicate the measuring points. The black dashed line roughly indicates the eastern margin of the Central Range. Areas enclosed by red lines with the marks of I, II, III, and IV is the four regions with high geothermal gradients. The GG' line indicates the location of the temperature structure which are shown in (b). (For interpretation of the references to colour in this figure legend, the reader is referred to the web version of this article.)

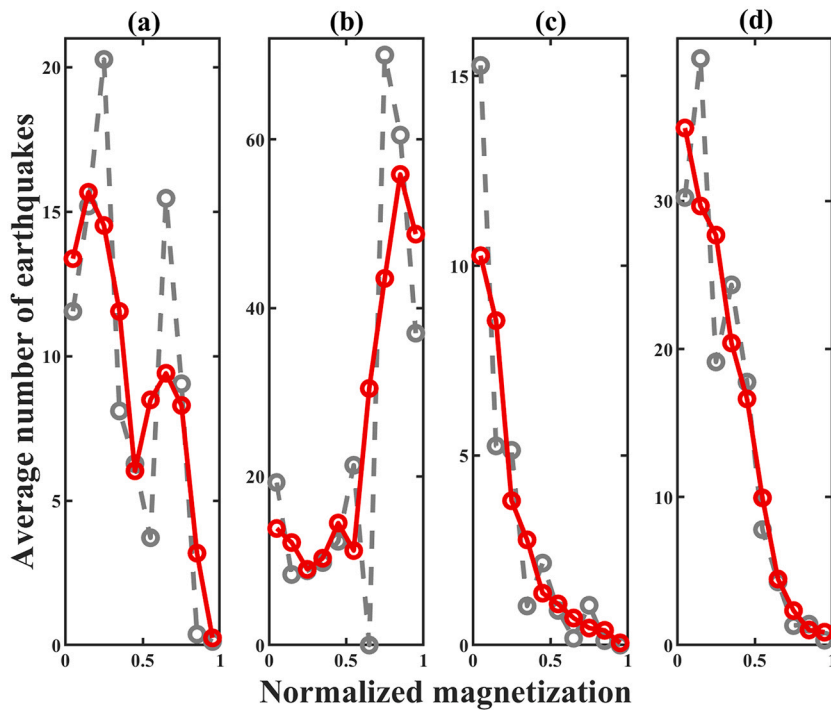


**Fig. 11.** The relationships between the average number of earthquakes and normalized magnetization in the four regions with high geothermal gradients. The relationships in the region I, II, III, and IV are shown in (a), (b), (c) and (d), respectively. In each subgraph, the gray dashed line represents the original relationship; the red solid line represents the relationship after the three-point moving average. (For interpretation of the references to colour in this figure legend, the reader is referred to the web version of this article.)

lateral changes in the P-wave velocity. This suggests that earthquake distributions are not only governed by the strength of rocks but also by other geophysical parameters. Significant lateral changes beneath the four aseismic regions can be observed in the magnetization structure. Earthquakes roughly distribute away from the relatively-high level magnetizations. It suggests that the magnetization would be an additionally promising parameter dominating earthquake locations.

In terms of the FF' profile (Fig. 8), the relationships among the P-wave velocity, the magnetization, and earthquake locations are unclear due to complex geological structure. The eastern margin is the youngest part of Taiwan that formed in the Neocene (Table 1), a series of volcanic islands lie on the Philippine Sea Plate that moves northward to Taiwan Island at a rate of 8.2 mm/y (Yu et al., 1997). Materials with a relatively-high level of magnetization roughly located at from 12 km to 40 km in depth (Fig. 8b) that is mainly caused by the igneous rocks formed by the cooling and precipitation of the intruded magma. P-wave velocity shows a relatively-high level underlying the eastern margin of Taiwan (Fig. 8c). Earthquakes around the FF' profile roughly distribute in areas with relatively-low magnetization and relatively-low level of P-wave velocity. An obvious exception, which earthquakes locate close to areas with a relatively-high level of magnetization and P-wave velocity (Fig. 8b and c), is found in the northern part of the FF' profile. Complex results suggest that multiple parameters dominate earthquake locations.

#### 4. Discussion

Earthquakes seem to occur away from strata with relatively-high magnetization in the studied profiles. We further examine the relationship between the magnetization from the inversion results and earthquakes with magnitudes are greater than or equal to 2 occurring in onshore Taiwan Island between 1991 and 2017. We normalized the magnetization by using the difference between the maximum and the minimum to mitigate the discrepancy in ranges of the magnetization values underlying distinct examined regions for faire comparison. The normalized magnetizations were further classified into 10 groups from 0 to 1 with an interval of 0.1. We computed the average number of earthquakes from the total count in each grid with the normalized magnetization that belongs to a particular classified group. The

proportional relationships suggest that earthquakes occur away from strata with relatively-low magnetization. In contrast, the inversely proportional relationships suggest that earthquakes occur away from strata with relatively-high magnetization. In the west of Taiwan, the average number of earthquakes is inversely proportional to the normalized magnetization (Figs. 1a and 9). The inversely proportional relationship roughly agrees with the observation from the profiles (Figs. 3-7). However, the average number is roughly proportional to the normalized magnetization in the east of Taiwan (Figs. 1a and 9). We further examine the relationship associated with the suture zone (Chen, 2008) around the FF' profile (Figs. 1b and 9), and the inversely proportional relationship can be found with the normalized magnetization between 0.15 and 0.45. In contrast, the proportional relationship is observed for the normalized magnetization ranged between 0.45 and 0.95. The analytical results around the FF' profile comprise the relationships from the both sides of it due to the suture zone. This suggests that the opposite relationships from the west and east of Taiwan should be the fact and other factors would dominate earthquake distribution.

Fig. 10a shows the reproduced data of the geothermal gradients from Lee and Cheng (1986) in Taiwan. The geothermal gradients in the west of Taiwan are generally lower than them in the east (also see Chen, 2008). The difference of the geothermal gradients in the west and east of Taiwan suggests that the subsurface temperature would be one of the potential factors dominating earthquake distribution. We examine the relationship between the earthquake numbers and the magnetization underlying the four regions (marked by I, II, III, and IV in Fig. 10a) with relatively-high geothermal gradients around the FF' profile. The inversely proportional relationships between the average number of earthquakes and the normalized magnetization were found in the region I, III, and IV (Fig. 11a, c, d) that agree with what is observed in the west of Taiwan. For the region II, the average number of earthquakes is roughly proportional to the normalized magnetization (Fig. 11b). To expose the causal mechanism behind, we further examine the relationship between the normalized magnetization and the average number of earthquakes for the strata from the surface to the bottom boundary varying from 3 km to 45 km with a step of 3 km (Fig. S6) beneath the region II. The inversely proportional relationship between the average number of earthquakes and the normalized magnetization gradually

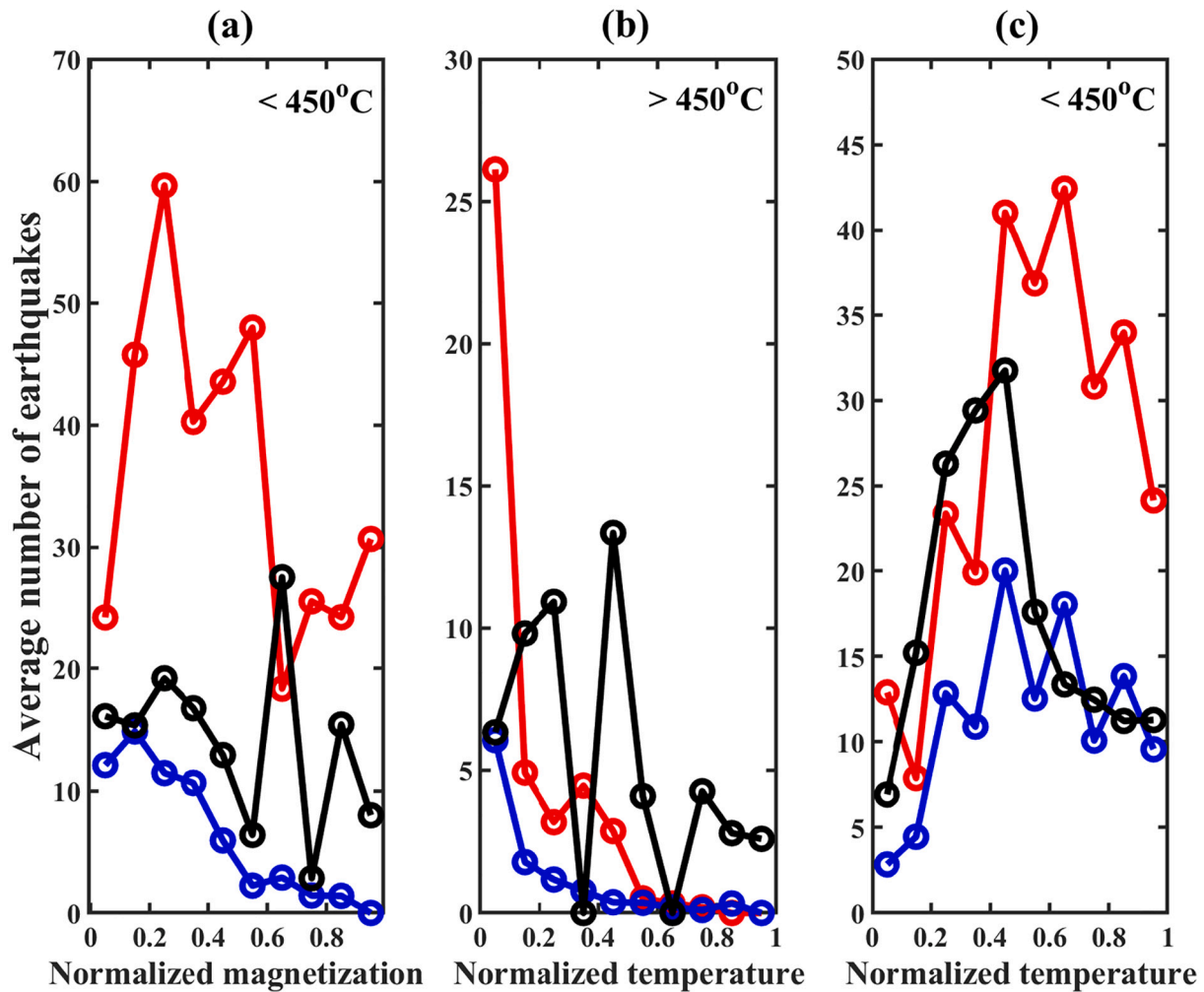


**Fig. 12.** The relationships among the average number of earthquakes, the normalized magnetization and the normalized temperature. (a) shows the relationship between the average number of earthquakes and the normalized magnetization for the depths with the subsurface temperature is lower than  $450^{\circ}\text{C}$  in the west (blue line), the east (red line), and the Central Range (black line) of Taiwan, respectively. (b) shows the relationship between the average number of earthquakes and the normalized temperature for the depths with the subsurface temperature is greater than  $450^{\circ}\text{C}$  in the west (blue line), the east (red line), and the Central Range (black line) of Taiwan, respectively. (c) shows the relationship between the average number of earthquakes and the normalized temperature for the depths with the subsurface temperature is lower than  $450^{\circ}\text{C}$  in the west (blue line), the east (red line), and the Central Range (black line) of Taiwan, respectively. (For interpretation of the references to colour in this figure legend, the reader is referred to the web version of this article.)

disappears at the depth of  $15 \pm 3$  km (Fig. S6). This suggests that the inversely proportional relationship certainly exists in the shallow depth but the subsurface temperature dominates earthquake in the deep depth.

We retrieved the subsurface temperature (Fig. 10b) along the GG' profile (Fig. 10a) from the numerical model proposed in Simoes et al. (2007). The temperature underlying the region II is  $\sim 450^{\circ}\text{C}$  at the depth of 15 km. We thus re-examine the relationship between the normalized magnetization and the average number of earthquakes for the depths with subsurface temperature is lower than  $\sim 450^{\circ}\text{C}$  in the three study regions (i.e., the west and east of Taiwan and the Central Range with the numerical model proposed in Simoes et al., 2007). Note that the estimation of the depth with the temperature  $\sim 450^{\circ}\text{C}$  for exterior areas of the numerical model proposed in Simoes et al. (2007) is based on an assumption of  $0^{\circ}\text{C}$  in the subsurface with a constant value of the geothermal gradient from Lee and Cheng (1986). The average number of earthquakes is inversely proportional to the normalized magnetization for the underlying strata from subsurface to the depth of the temperature threshold in the three regions (Fig. 12a). In contrast, the temperature replaces the magnetization to examine the relationship between the average number of earthquakes and the normalized temperature by using the same method for the underlying strata which is deeper than

the depth of the temperature threshold to the bottom (i.e., 45 km) in the three regions. The average number of earthquakes is inversely proportional to the normalized temperature, which is also obtained in the three regions (Fig. 12b). The problems of the opposite relationships in Figs. 9 and 10 can be partially resolved when the temperature threshold of  $\sim 450^{\circ}\text{C}$  is considered. We further examine the average number of earthquakes and the normalized temperature which is lower than the threshold of  $\sim 450^{\circ}\text{C}$  and the results are shown in Fig. 12c. However, the average numbers increase with the normalized temperature of  $< \sim 0.5$  which is different from the common sense. Scott et al. (2015) found that the brittle to ductile transition temperature  $450^{\circ}\text{C}$  is a critical temperature controlling the formation of supercritical resources. This suggests that earthquake distributions are dominated by the subsurface temperature of  $> \sim 450^{\circ}\text{C}$  when the rocks transform from brittle to ductile.

## 5. Conclusion

The strength of rocks is the major factor that governs earthquake locations. However, earthquakes usually cluster in particular regions without obvious lateral changes in the P-wave velocity. Earthquakes mainly distribute away from areas with a relatively-high level of

magnetization when subsurface temperature is lower than  $\sim 450$  °C. When subsurface temperature is greater than  $\sim 450$  °C, earthquakes roughly locate in strata with relatively-low level of temperature. Magnetization and subsurface temperature dominate earthquake locations when rocks are brittle and ductile, respectively. Earthquake locations are governed by the well-known factor of the strength of rocks accompanying with the magnetization and subsurface temperature. Investigations of the magnetization and temperature underground provide an opportunity to understand the earthquake distributions, which is advantageous in conducting risk assessments of the occurrence of earthquakes.

### Declaration of Competing Interest

We declare that we have no financial and personal relationships with other people or organizations that can inappropriately influence our work, there is no professional or other personal interest of any nature or kind in any product, service and/or company that could be construed as influencing the position presented in, or the review of, the manuscript entitled, "The relationship among earthquake location, magnetization, and subsurface temperature beneath the Taiwan areas".

### Acknowledgements

This work is supported by the Joint Funds of the National Natural Science Foundation of China (Grant no. U2039205), Ministry of Science and Technology of Taiwan (Grants No. MOST 105-2116-M-008-014- , MOST 106-2119-M-008-010- , MOST 106-2116-M-194-016- and MOST 106-2628-M-008-002), and the Sichuan earthquake Agency-Research Team of GNSS based geodetic tectonophysics and mantle-crust dynamics of the Chuan-Dian region (Grant No. 201804).

### Appendix A. Supplementary data

Supplementary data to this article can be found online at <https://doi.org/10.1016/j.pepi.2021.106800>.

### References

- Barton, C.E., 1997. International geomagnetic reference field: the seventh generation. *J. Geomagn. Geoelectr.* 49, 123–148.
- Bassett, D., Watts, A.B., 2015. Gravity anomalies, crustal structure, and seismicity at subduction zones: 1. Seafloor roughness and subducting relief. *Geochem. Geophys. Geosyst.* 16 (5), 1508–1540.
- Chang, W.Y., Chen, K.P., Tsai, Y.B., 2016. An updated and refined catalog of earthquakes in Taiwan (1900–2014) with homogenized mw magnitudes. *Earth Planets Space* 68, 45. <https://doi.org/10.1186/s40623-016-0414-4>.
- Chen, P.Y., 2008. *Taiwan Geology*. Taiwan Applied Geology Guild, Taiwan.
- Chen, C.S., Chen, C.C., 2000. Magnetotelluric soundings of the source area of the 1999 chi-chi earthquake in Taiwan. Evidence of fluids at the hypocenter. *Terr. Atmos. Ocean. Sci.* 11 (3), 679–688.
- Chen, K.J., Wang, C.M., Hsu, S.K., Liang, W.T., 2001. Geomagnetic basement relief of the northern Taiwan area. *Terr. Atmos. Ocean. Sci.* 12 (3), 441–460.
- Chen, C.H., Chen, C.R., Sun, S., Wen, S., Du, J.S., Lin, C.H., Huang, Y.H., Han, P., Liu, J. Y., 2021. Novel approaches of magnetic inversion using seismic tomography in Taiwan area. *Phys. Earth Planet. Inter.* 312, 106663. <https://doi.org/10.1016/j.pepi.2021.106663>.
- Deschamps, A., Monie, P., Lallemand, S., Hsu, S.K., Yeh, K.Y., 2000. Evidence for early cretaceous oceanic crust trapped in the Philippine Sea plate. *Earth Planet. Sci. Lett.* 179, 503–516.
- Doo, W.B., Hsu, S.K., Armada, L., 2015. New magnetic anomaly map of the East Asia with some preliminary tectonic interpretations. *Terr. Atmos. Ocean. Sci.* 26 (1), 73–81.
- Hansen, P.C., O'Leary, D.O., 1993. The use of the L-curve in the regularisation of discrete ill-posed problems. *SIAM J. Sci. Comput.* 14, 1487–1503.
- Hasegawa, A., Yamamoto, A., 1994. Deep, low-frequency microearthquakes in or around seismic low-velocity zones beneath active volcanoes in northeastern Japan. *Tectonophysics* 233 (3–4), 233–252.
- Hornig, C.S., Laj, C., Lee, T.Q., Chen, J.C., 1992. Magnetic characteristics of sedimentary rocks from the Tsengwen-chi and Erhjen-chi section in southwestern Taiwan. *Terr. Atmos. Ocean. Sci.* 3, 519–532.
- Hsieh, H.H., Chen, C.H., Lin, P.Y., Yen, H.Y., 2014. Curie point depth from spectral analysis of magnetic data in Taiwan. *J. Asian Earth Sci.* 90, 26–33. <https://doi.org/10.1016/j.jseas.2014.04.007>.
- Hsu, S.K., Sibuet, J.C., 1995. Is Taiwan the result of arc-continent or arc-arc collision? *Earth Planet. Sci. Lett.* 136, 315–324. [https://doi.org/10.1016/0012-821X\(95\)00190-N](https://doi.org/10.1016/0012-821X(95)00190-N).
- Hsu, S.K., Liu, C.S., Shyu, C.T., Liu, S.Y., Sibuet, J.C., Lallemand, S., Wang, C., Reed, D., 1998. New gravity and magnetic anomaly maps in the Taiwan-Luzon region and their preliminary interpretation. *Terr. Atmos. Ocean. Sci.* 9, 509–532.
- Hsu, S.K., Yeh, Y.C., Lo, C.L., Lin, A.T.S., Doo, W.B., 2008. Link between crustal magnetization and earthquakes in Taiwan. *Terr. Atmos. Ocean. Sci.* 19 (5), 445–450.
- Ikari, M.J., Kameda, J., Saffer, D.M., Kopf, A.J., 2015. Strength characteristics of Japan trench borehole samples in the high-slip region of the 2011 Tohoku-Oki earthquake. *Earth Planet. Sci. Lett.* 412, 35–41.
- Konstantinou, K.I., Lin, C.H., Liang, W.T., 2007. Seismicity characteristics of a potentially active quaternary volcano: the Tatun volcano group, northern Taiwan. *J. Volcanol. Geotherm. Res.* 160, 300–318. <https://doi.org/10.1016/j.jvolgeores.2006.09.009>.
- Lacombe, O., Mouthereau, F., Angelier, J., Defontaine, B., 2001. Structural, geodetic and seismological evidence for tectonic escape in SW Taiwan. *Tectonophysics* 333, 323–345.
- Leary, P.C., 1997. Rock as a critical-point system and the inherent implausibility of reliable earthquake prediction. *Geophys. J. Int.* 131 (3), 451–466.
- Lee, C.J., 1996. The Hydrocarbon Exploration on Tertiary Strata in Taiwan. Research Development Report, 85008, Ministry of Economic Affairs.
- Lee, C.R., Cheng, W.T., 1986. Preliminary heat flow measurements in Taiwan. In: *Proceedings of the Forth Circum-Pacific Energy and Mineral Resources Conference*, Singapore.
- Lee, C.J., Din, S.H., 1993. The geological logging data analysis and explanation. In: *Ann. Report of CPC Corporation*, Taiwan, 57.
- Li, Y., Oldenburg, D.W., 1996. 3-D inversion of magnetic data. *Geophysics* 61, 394–408.
- Li, Y., Oldenburg, D.W., 2003. Fast inversion of large-scale magnetic data using wavelet transforms and a logarithmic barrier method. *Geophys. J. Int.* 152, 251–265. <https://doi.org/10.1046/j.1365-246X.2003.01766.x>.
- Li, Z.L., Yao, C.L., Zheng, Y.M., Wang, J.H., Zhang, Y.W., 2018. 3D magnetic sparse inversion using an interior-point method. *Geophysics* 83, J15–J32.
- Lin, C.H., 2000. Thermal modeling of continental subduction and exhumation constrained by heat flow and seismicity in Taiwan. *Tectonophysics* 324, 189–201.
- Lin, A.T., Watts, A.B., Hesselbo, S.P., 2003. Cenozoic stratigraphy and subsidence history of the South China Seamargin in the Taiwan region. *Basin Res.* 15, 453–478. <https://doi.org/10.1046/j.1365-2117.2003.00215>.
- Luo, Y., Yao, C., 2007. Theoretical study on cuboid magnetic field and its gradient expression without analytic singular point. *Oil Geophys. Prospect.* 42, 714–719 (in Chinese with English abstract).
- Nagel, S., Castellort, S., Wetzel, A., Willett, S.D., Mouthereau, F., Lin, A.T., 2013. Sedimentology and foreland basin paleogeography during Taiwan arc continent collision. *J. Asian Earth Sci.* 62, 180–204. <https://doi.org/10.1016/j.jseas.2012.09.001>.
- Nakatsuka, T., Okuma, S., Morijiri, R., Makino, M., 2005. Compilation of airborne magnetic anomaly maps in Japan from the variety of surveys with long epoch differences. In: *Proc. 11th IAGA Workshop on Magnetic Obs.*, pp. 230–233.
- Pilkington, M., 1997. 3-D magnetic imaging using conjugate gradients. *Geophysics* 62, 1132–1142. <https://doi.org/10.1190/1.1444214>.
- Regan, R.D., Cain, J.C., 1975. The use of geomagnetic field models in magnetic surveys. *Geophysics* 40, 621–629. <https://doi.org/10.1190/1.1440553>.
- Scott, S., Driesner, T., Weis, P., 2015. Geologic controls on supercritical geothermal resources above magmatic intrusions. *Nat. Commun.* 6 (1), 1–6.
- Sibuet, J.C., Hsu, S.K., 1997. Geodynamics of the Taiwan arc-arc collision. *Tectonophysics* 274, 221–251.
- Simoes, M., Avouac, J.P., Beyssac, O., Goffe, B., Farley, K.A., Chen, Y.G., 2007. Mountain building in Taiwan: a thermokinematic model. *J. Geophys. Res.* 112, B11405. <https://doi.org/10.1029/2006JB004824>.
- Singh, S.C., Hananto, N., Mukti, M., Robinson, D.P., Das, S., Chauhan, A., Carton, H., Gratacos, B., Midnet, S., Djajadhardja, Y., Harjono, H., 2011. Aseismic zone and earthquake segmentation associated with a deep subducted seamount in Sumatra. *Nat. Geosci.* 4 (5), 308–311.
- Suppe, J., 1981. Mechanics of mountain building and metamorphism in Taiwan. *Mem. Geol. Soc. China* 4, 67–89.
- Tang, C.H., Hsu, Y.J., Sylvain, B., Moore, J.D.P., Chang, W.L., 2019. Lower-crustal rheology and thermal gradient in the Taiwan orogenic belt illuminated by the 1999 chi-chi earthquake. *Sci. Adv.* 5. <https://doi.org/10.1126/sciadv.aav3287> eav3287.
- Tarasov, B.G., Randolph, M.F., 2011. Superbrittleness of rocks and earthquake activity. *Int. J. Rock Mech. Min.* 48 (6), 888–898.
- Tong, L.T., Ouyang, S., Guo, T.R., Lee, C.R., Hu, K.H., Lee, C.L., Wang, C.J., 2008. Insight into the geothermal structure in Chingshui, Ilan, Taiwan. *Terr. Atmos. Ocean. Sci.* 19, 413–424. [https://doi.org/10.3319/TAO.2008.19.4.413\(T\)](https://doi.org/10.3319/TAO.2008.19.4.413(T)).
- Tsai, Y.B., Hsiung, Y.M., Liaw, H.B., Lueng, H.P., Yao, T.H., Yeh, Y.H., Yeh, Y.T., 1974. A seismic refraction study of eastern Taiwan. *Petro. Geol. Taiwan* 11, 165–185.
- Wang, C., Huang, C.P., Ke, L.Y., Chien, W.J., Hsu, S.K., Shyu, C.T., Cheng, W.B., Lee, C.S., Teng, L.S., 2002. Formation of the Taiwan island as a solitary wave the Eurasian continental plate margin: magnetic and seismological evidence. *Terr. Atmos. Ocean. Sci.* 13, 339–354.
- Whitcomb, J.H., Garmany, J.D., Anderson, D.L., 1973. Earthquake prediction: variation of seismic velocities before the San Francisco earthquake. *Science*. 180 (4086), 632–635.
- Yen, H.Y., Yeh, Y.H., Wu, F.T., 1998. Two-dimensional crustal structures of Taiwan from gravity data. *Tectonics* 17, 103–111.
- Yen, H.Y., Chen, C.H., Hsieh, H.H., Lin, C.R., Yeh, Y.H., Tsai, Y.B., Liu, J.Y., Yu, G.K., Chen, Y.R., 2009. Magnetic survey of Taiwan and its preliminary interpretations.

- Terr. Atmos. Ocean. Sci. 20, 309–314. [https://doi.org/10.3319/TAO.2008.04.08.01\(T\)](https://doi.org/10.3319/TAO.2008.04.08.01(T)).
- Yu, S.B., Tsai, Y.B., 1979. Geomagnetic anomalies of the Ilan plain, Taiwan. *Pet. Geol. Taiwan* 16, 19–27.
- Yu, S.B., Chen, H.Y., Kuo, L.C., 1997. Velocity field of GPS stations in the Taiwan area. *Tectonophysics* 274, 41–59.
- Zhang, X., Hu, X.F., Shen, J.X., Zhao, L., Liu, M., 1995a. Relation of apparent magnetization intensity distribution in Sichuan Basin and the earthquake region on its western margin to seismogenic environment. *North China Earthq. Sci.* 13 (1), 17–22.
- Zhang, X., Hu, X.F., Liu, M., Shen, J.X., Zhao, L., He, W.M., 1995b. Study on the distribution of apparent magnetization intensity and its relation to earthquakes in Tangshan-Luanxian earthquake region. *J. Seismol. Res.* 18 (1), 63–67.